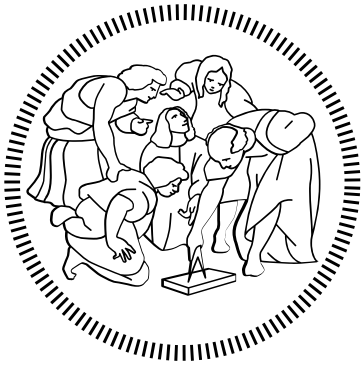

POLITECNICO
MILANO 1863

Reverse Engineering of Juno Mission

Homework 2

Course of Space System Engineering & Operations
Academic Year 2023-2024

Group 5

Alex Cristian Turcu	alexcristian.turcu@mail.polimi.it	10711624
Chiara Poli	chiara3.poli@mail.polimi.it	10731504
Daniele Paternoster	daniele.paternoster@mail.polimi.it	10836125
Marcello Pareschi	marcello.pareschi@mail.polimi.it	10723712
Paolo Vanelli	paolo.vanelli@mail.polimi.it	10730510
Riccardo Vidari	riccardo.vidari@mail.polimi.it	10711828

Contents

Notation

ME	Main Engine
RCS	Reaction Control System
DSM	Deep Space Manoeuvre
DSN	Deep Space Network
OTM	Orbit Trim Manoeuvre
TCM	Trajectory Correction Manoeuvre
SK	Station Keeping
PRM	Period Reduction Manoeuvre
JOI	Jupiter Orbit Insertion
REM	Rocket Engine Module
MEF	Main Engine Flush
TRL	Technology Readiness Level
RW	Reaction Wheel
COM	Centre Of Mass
MAG	Magnetometer
PC	Plane Change
ELA	Earth Look Angle
EGA	Earth Gravity Assist
FB	Fly-by
$\mathbf{INJ_J}$	Jupiter injection
$\mathbf{ESC_E}$	Earth escape
TLGA	Toroidal Low Gain Antenna
HGA	High Gain Antenna
SEP	Sun-Earth-Probe
PED	Propellant Expulsion Device
τ	Burn time [s]
ΔV	Velocity change [m/s]
v_∞	Asymptotic velocity [m/s]
μ_J	Jupiter planetary constant [km^3/s^2]
r_p	Radius of pericentre [km]
e_{cap}	Eccentricity of capture orbit [-]
NTO	Nitrogen Tetroxide
O/F	Oxidizer to Fuel ratio
M_{dry}	Total dry mass of satellite [kg]
M_{launch}	Total mass of satellite at launch [kg]
M	Total mass of satellite [kg]
M_p	Total mass of propellants [kg]
M_f	Total mass of fuel [kg]
M_{ox}	Total mass of oxidizer [kg]
M_{He}	Total mass of helium [kg]
V_{He}	Total volume of helium [m^3]
I_s	Specific impulse [s]
g_0	Standard gravitational acceleration [m/s^2]
r_{tank}	Radius of spherical propellants tanks [m]
p_{tank}	Pressure of propellants tanks [Pa]
T_{tank}	Temperature of propellants tanks [K]
t_{tank}	Thickness of propellants tanks [m]
V_{tank}	Volume of one empty propellants tank [m^3]
M_{tank}	Mass of one empty propellants tank [kg]
$r_{tank,He}$	Radius of cylindrical helium tanks [m]
$h_{tank,He}$	Height of cylindrical helium tanks [m]
$t_{tank,He}$	Thickness of helium tanks [m]
$M_{tank,He}$	Mass of one empty helium tank [kg]
R_{He}	Specific gas constant for helium [J/kg·K]
γ_{He}	Adiabatic index for helium [-]
Ti6Al4V	Titanium alloy
Al7075	Aluminum alloy
ρ	Density of the material [kg/m^3]
σ	Tensile yield strength of the material [Pa]

1 Mission analysis and ΔV budget

1.1 Rationale of the mission analysis

The mission analysis previously described could be split into two macro-phases:

- from launch to the interplanetary transfer, including DSMs and the Earth fly-by;
- planetary phase around Jupiter.

The main objectives of the mission analysis were to keep the overall launch energy C_3 and deterministic ΔV as low as possible, compliant with the constraints imposed by the navigation and spacecraft operational requirements. Regarding the interplanetary transfer, two main options were available, both including an EGA. The first option, named as "$2 - dV\,EGA$", contemplated a launch window time frame in October-November 2011. However, the latter was discarded since the approach angle at Jupiter would have resulted in a latitude farther away from the equator. This would have brought to higher radiation levels, hence a reduced time available for the science operations[1]. The second option, named as "$2 + dV\,EGA$", contemplated a launch window time frame in August 2011 and it ended up being the chosen one. A viable back-up for this transfer would have happened in October 2012, since the basic features of "$2 + dV\,EGA$" repeat every 13 months. Regarding the interplanetary trajectory constraints, they could be divided into three categories:

- **Launch energy C_3 and timing constraints.** Fixing an initial value for the energy provided by the launcher, different possibilities of departure date could be analyzed. Every launch date defined a trajectory that was characterized by a required C_3 and deterministic ΔV. The maximum $C_3 = 31.1$ km^2/s^2 was defined by the Atlas V551 launcher[2]. Analyzing Juno's ephemeris for the actual launch date, the calculated value is $C_3 = 31.08$ km^2/s^2. The trajectory reconstructed through the optimization problem and explained in subsection 1.2, revealed a value of $C_3 = 29.34$ km^2/s^2, with departure date on 18$^{\text{th}}$ August 2011. Restricting the launch window domain around 5$^{\text{th}}$ August 2011 (the actual one) the value is $C_3 = 30.40$ km^2/s^2. In the non-restricted window for departure, the trend of the C_3 over time can be evaluated in the work of Kowalkowski and Lam[1].
- **Interplanetary events.** The milestones of this phase were DSMs and EGA. The fly-by was constrained to happen at a fixed altitude of 800 km well above ISS, but it could be lowered up to 500 km. This last decrease of the altitude value could have improved the robustness of the trajectory in the case of eventual delays in DSMs, decreasing also the ΔV of the mission and the intensity of the radiation at Jupiter arrival[3]. However, the most challenging task was the selection of the DSM dates, in fact this choice would have affected the required launch C_3 and overall mission ΔV[1]. Moreover, DSM had to be split into two equally lasting burns, separated by two days. This was dictated by engine capabilities, described in subsection 2.1. As precaution, due to anomalous pressure and temperature values of the oxidizer feeding line during DSM-1, the two manoeuvres ended up being performed two weeks apart. An additional problem arose from the $2 + dV\,EGA$ interplanetary structure and the needs to perform the DSM at aphelion while having real-time visibility. This constraint was set up by imposing a SEP angle greater than 10° for acquisition of data, and SEP angle greater than 3° for execution of the manoeuvre. This difference was due to the need of seven days to plan the manoeuvre on ground after the necessary two days of data collection. In the eventuality of a burn before solar conjunction, an adequate time to retry failed attempts was considered. Another constraint regarding telecommunications and navigation was due to the positioning of the toroidal antenna (TLGA) which is used for ground link in the early phases and is mounted on the aft deck and aligned with the -Z-axis, as shown in Figure 2. To ensure a good signal with this antenna, the ELA was constrained to be within ± 10° around 90°: since Doppler data is of very little value when ELA is too close to 90°, the combined range for the ELA resulted to be of 80° ÷ 87° and 93° ÷ 100°.
- **Jupiter arrival timing and geometry.** Jupiter arrival and insertion was constrained by multiple aspects. First of all, since a direct injection into the science orbit would have been too expensive, the burn was split into two manoeuvres (JOI and PRM), saving over 170 m/s[1] related to gravity losses. In order to avoid longitudes at which the magnetic field is stronger, JOI and PRM dates had to be accurately selected. In addition, due to the critical nature of JOI, the manoeuvre had to take place during the overlapping coverage of two DSN complexes. Since the longest one was provided by Goldstone-Canberra, the burn and pre-burn events had to happen during that time frame. As far as PRM was concerned, dual DSN coverage was not required. However, the optimal date for PRM could be selected in order to minimize the overall ΔV and to manoeuvre at lower magnetic field longitudes. Lastly, the perijove was bounded to be at distances higher than 4500 km over the 1 bar pressure level of the atmosphere, allowing to operate in the hole of the torus that describes the highest radiation levels.

1.2 Simulation of the interplanetary trajectory

To reconstruct the interplanetary phase, a simulation was set up in *Matlab*. The implemented model considered three heliocentric legs, linked with the patched-conics method:

- from Earth to DSM position;

- from DSM position to fly-by at Earth;
- from fly-by position to Jupiter.

In order to minimize the total ΔV of the mission, a cost function was defined. This is determined by the sum of four contributions:

- $\Delta V_{esc,E}$: escape from Earth heliocentric orbit into the first interplanetary leg;
- ΔV_{dsm}: deep space manoeuvre;
- ΔV_{fb}: burn manoeuvre at Earth's fly-by hyperbola pericentre;
- $\Delta V_{inj,J}$: injection into Jupiter's heliocentric orbit.

The calculations were based on analytical ephemeris for the planets and the Lambert method was used to design the paths. The implementation was constrained by various inputs, according to the development of the mission:

- Earth departure date, defined in the interval from 05/08/2011 to 26/08/2011
- DSMs condensed in one impulsive burn
- DSM date, from 20/08/2012 to 10/09/2012
- DSM position domain constrained by means of keplerian parameters from the real mission ephemeris
- Fly-by date, from 20/09/2013 to 20/10/2013
- Fly-by altitude, of at least 500 km
- Jupiter arrival date, from 20/06/2016 to 10/07/2016

Then a genetic algorithm was used to minimize the cost function and the match between the calculations and Juno ephemeris was verified as shown in Figure 1.

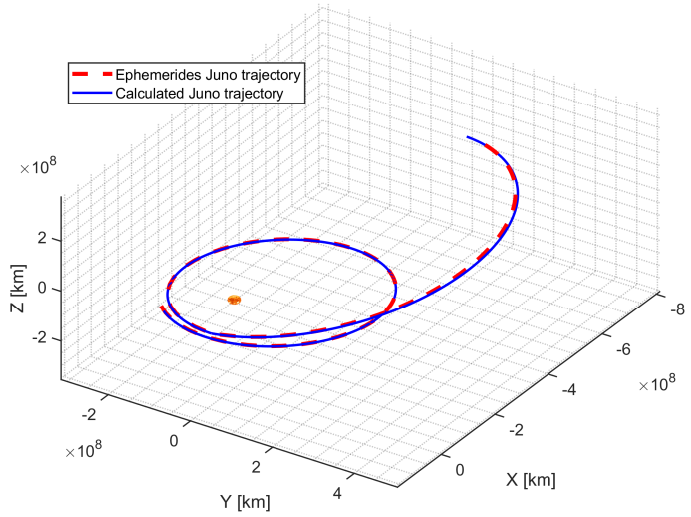

Figure 1: Comparison of trajectories

	ΔV [km/s]	Date
ESC$_E$	5.3920	14/08/2011
DSM	0.7225	29/08/2012
FB	$1.9872 \cdot 10^{-7}$	08/10/2013
INJ$_J$	5.4552	09/07/2016

Table 1: Calculated solution

The obtained results are coherent with the actual mission data[4]. Regarding Table 1, some values might seem particularly high in relation to the main engine capabilities. Indeed, not all of the ΔVs had to be performed by the main engine:

- $\Delta V_{esc,E}$ was executed by the upper stage of the Atlas V551, in the limits of the launcher performance C_3.
- $\Delta V_{inj,J}$ was due to the rendezvous at Jupiter. The only burn required to enter an elliptical orbit had to be given at the pericentre of the hyperbola. The impulsive ΔV can be calculated as follows, considering $e_{cap} = 0.9884$ and $r_p = 75237.6$ km in relation to the designed 107 days orbit:

$$\Delta V_{JOI} = v_\infty \left(\sqrt{1 + \frac{2\mu_J}{r_p v_\infty^2}} - \sqrt{\frac{\mu_J (1 + e_{cap})}{r_p v_\infty^2}} \right) = 424.07 \text{ m/s} \tag{1}$$

Moreover, the low ΔV_{fb} value in Table 1 indicates that gravity assist was not powered. Clean-up manoeuvre and TCMs were performed before and after the fly-by, hence this small burn.

1.3 ΔV budget

A summary of the planned, performed and simulated manoeuvres is exposed in Table 2. The design column is referred to the pre-launch schedule, while the performed column is relative to the actual mission. The designed mission never saw life since various problems occurred during the cruise phase: from a nominal capture orbit with a period of 107 days and a science orbit of 11 days, the new scheduled orbits were of 53.5 days and 14 days respectively.

For this precise reason the performed values differ from the design ones, especially the JOI, which was related to a different capture orbit, and the PC, which was not meant to be performed originally. The whole simulation has been performed on the designed 107 days orbit and the 11 days one. The final two columns show the required ME burn times for the designed and the performed mission respectively.

Manoeuvres	**Design** [m/s]	**Perf.** [m/s]	**Sim.** [m/s]	τ_{ME} **Design** [min]	τ_{ME} **Perf.** [min]
TCM-1 ÷ 2 (RCS)[5]	4.4	1.71	-	-	-
DSM-1 (ME)[5]	360.1	344.16	722.51	30.97	29.71
DSM-2 (ME)[5]	394.8	387.94		30.07	29.77
TCM-4 ÷ 15 (RCS)[5]	32.5	7.89	-	-	-
MEF (ME)[5]	3.3	3.3	-	-	-
JOI (ME)[6]	424.07 ^{I}	541.73	424.07	27.86	35.65
JOI clean-up (RCS)[6]	4.92	6.39	-	-	-
PRM (ME)[6]	636	-	602.45	35.19	-
OTM pre-PC (RCS)[7]	120 ^{II}	94.88	-	-	-
PC (RCS)	-	56.39	69.97 ^{III}	-	-
OTM post-PC (RCS)	-	108.08	-	-	-
De-Orbit (RCS)[8]	75 ^{IV}	30.89 ^{V}	87.93	-	-

Table 2: Overall mission budget and simulation

^{I} This value has been assumed equal to the one calculated from the insertion on the 107 days orbit.
^{II} This value assumes 30 nominal science orbits with a required ΔV of 4 m/s.
^{III} This value is referred to the plane change of the 53 days orbit as no other trajectories required this manoeuvre.
^{IV} This value is assumed equal between the 11 days orbit and the 14 days orbit.
^{V} This value has been updated from the nominal 75 m/s since the de-orbit manoeuvre will be performed from a 53 days orbit and not from a 14 days orbit.

2 Propulsion system architecture

The spacecraft axes are defined as shown in Figure 2: the spacecraft is spinning along the +Z-axis, aligned with the HGA. The +X-axis is aligned with the MAG boom while the +Y-axis is in the direction of cross product between +Z-axis and +X-axis.

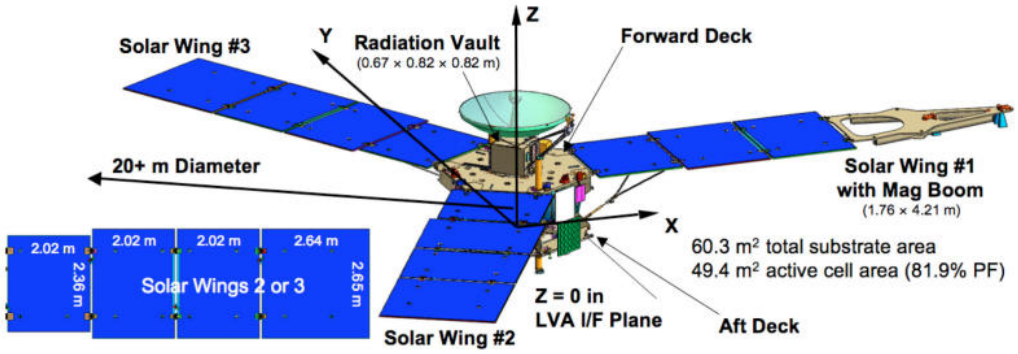

Figure 2: Axis description

2.1 Main Engine and RCS

Juno is equipped with a dual-mode propulsion system: the bi-propellant ME uses the hypergolic couple hydrazine and nitrogen tetroxide (N_2H_4–N_2O_4) while RCS uses hydrazine as monopropellant. This choice was made to simplify the design: fewer tanks are needed as fuel ones are shared between the two systems. Moreover, the choice of this specific hypergolic couple is dictated by the storage requirements of the mission: in a five-year cruise, reliability and sturdiness of the propulsive system were among the main drivers of the mission. Electric thrusters were discarded as TRL-9 technologies were required: other limitations such as power budget, an highly radioactive environment, weight and space inside the spacecraft required a more simple and light solution.

The ME is a Leros 1b, built by Nammo[9], which produces about 662 N of thrust with $I_{s,me}$ = 318.6 s. This particular engine is certified for a 42 minutes continuous burn and has a cumulative lifetime of 342 minutes, so the manoeuvres shown in Table 2 are compliant with this constraint. This engine is utilized during the DSMs, JOI and PRM. It is mounted inside the body of the spacecraft along the -Z-axis, centred between the propellant tanks and under the electronic vault. This solution has probably been adopted due to space requirements inside the Atlas V fairing and safety precautions during the cruise phase. The ME is also shielded by a hatch that opens when a manoeuvre is needed. The RCS is used for TCMs, attitude control and general SK. The catalyst used to decompose the hydrazine is the S-405, based on iridium and aluminum[10]. The whole RCS is composed by four REMs, each of them mounted along the ±Y-axis on a pylon, as shown in Figure 3. Every pylon houses three thrusters, the MR-111C by Aerojet Rocketdyne[11], pointed in different directions, each providing a thrust of 4.5 N with $I_{s,rcs}$ = 220 s. Electrical power is required to operate the feeding valves, heating valves and the catalytic bed, amounting to a maximum of around 13 W[12].

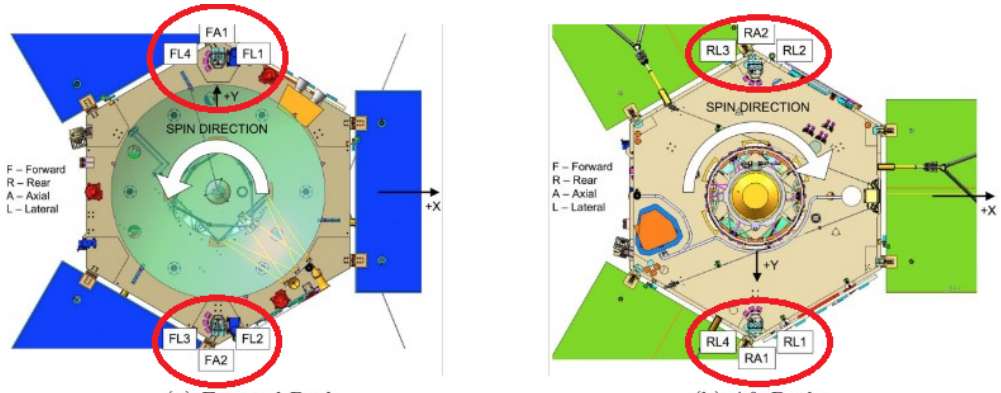

(a) Forward Deck (b) Aft Deck

Figure 3: Forward and Aft deck view

The pylons are raised respectively by 74 cm on the forward deck and about 26 cm on the aft deck as shown in Figure 4. With the need of limiting even more the interaction of the exhaust gasses with the on board instruments, the HGA and solar panels, axial thrusters are canted 10° away from the Z-axis while the lateral thrusters are canted 5° away from the X-axis and 12.5° toward the Z-axis[5]. This particular configuration of RCS is required since no RW nor any other type of active attitude control is present on the spacecraft: the ability of decoupling the forces and the momentum was thus needed. Lateral thrusters are denominated with letter "L" while axial thrusters are denominated with letter "A", as can be seen both from Figure 3 and Figure 4. This configuration increased the overall sturdiness of the propulsion system as "A" thrusters could be used as replacement of the ME for small manoeuvres. A simplified scheme of the propulsion system has been developed in Figure 5.

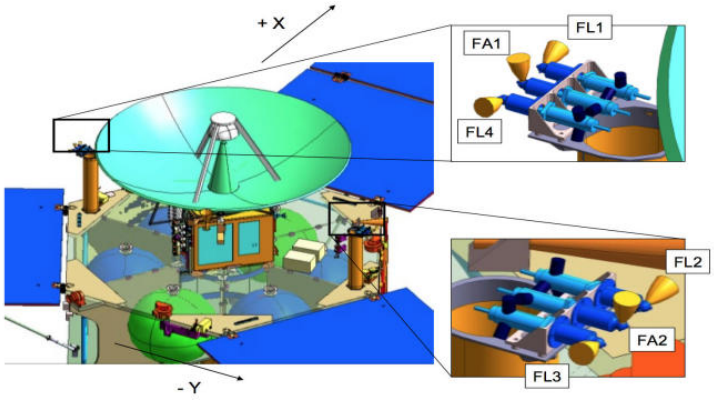

Figure 4: RCS Forward mount

2.2 Manoeuvre Implementation Modes

Juno's manoeuvres can be performed in two different modes: *vector-mode* and *turn-burn-turn*.
The *vector-mode* consists of separated and coordinated axial and lateral burns from RCS thrusters. As seen in subsection 2.1, the thrusters are not exactly perpendicular one to the other, so during a *vector-mode* manoeuvre an induced axial ΔV is generated and must be compensated.
The *turn-burn-turn* mode consists in a sequence of RCS and ME burns: first the spacecraft slews to the design spinning rate of 5 RPM, then the ME is ignited and the manoeuvre is performed. At last, the spacecraft slews back to its nominal spinning rate. This mode is used during all the ME burns. In this kind of manoeuvre the RCS uses the "L" thrusters on the REMs.

2.3 Tanks

Juno's tanks are equally distributed throughout its hexagonal shaped body. Four tanks are needed to store hydrazine and two tanks are needed to store the oxidizer. As can be seen from Figure 4, the oxidizer ones (green tanks) are located along the X-axis, while fuel ones (blue ones) are placed in the remaining bays. All six tanks work at 2.15 MPa, estimated as the sum of the nominal operational pressure of the ME and a small amount, 50 kPa, induced by the pressure losses of the system[9]. On board tanks have a sphere-like shape: it allows to have the most internal volume with the lowest possible surface and so both weight and heat exchange are limited.

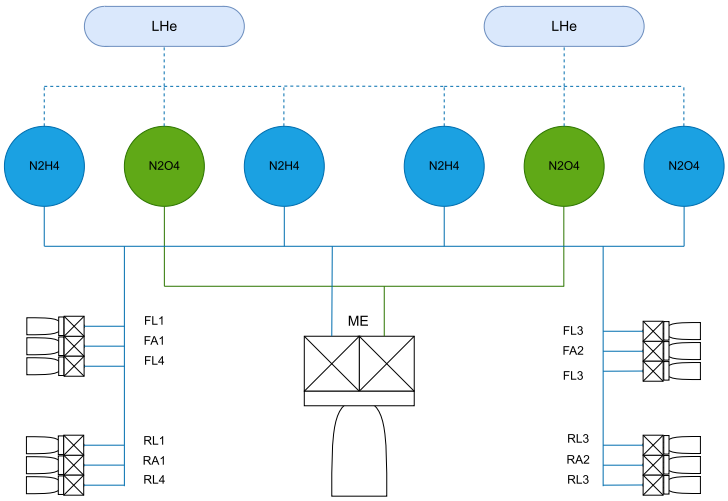

Figure 5: Propulsion system architecture

The two tanks[13] containing the supercritical helium needed to pressurize the propellant system are assumed to be initially pressurized at 21.5 MPa, a value ten times higher than the nominal working pressure, and are placed near solar wing one and solar wing two. Unlike fuel and oxidizer tanks, helium ones do not have a sphere-like shape due to volume management inside the bays[14]: cylindrical tanks allow to fill better the gaps present under the main tanks. The positioning of the pressurizer tanks breaks even more the symmetry of the mass distribution: this feature, in concomitance with the distribution of the propellant tanks, will make the COM shift not only along the Z-axis unless other precautions were made in placing other internal components.

A system of valves regulates the pressure inside the tanks to allow nominal operations of the ME and RCS. All the tanks are insulated from their surroundings and heating elements are present on both tanks and feeding lines to ensure safe and nominal temperature inlet for the whole propulsion system. One of the main problem with managing liquid in space is the need of guiding the propellants to the feeding lines of the engines to avoid mixture of gas and liquids during the injection in the combustion chamber, compromising the correct functioning of the propulsion system. Moreover, liquid propellants produce sloshing movements that could apply forces and moments inside the tanks, causing an unsteady oscillatory spin. Juno is a spin-stabilized spacecraft so the induced forces would cause a movement of nutation. A Propellant Expulsion Device (PED) is thus needed: the spinning of the spacecraft helps guiding the propellant to the most exterior part of the tanks were feeding lines are located[15]. MEFs are tasks needed to flush the main propellant line in order to test the system after a long period of rest. In order to accomplish its mission, Juno holds about 2000 kg of propellant: about 1280 kg of fuel and 720 kg of oxidizer[5]. A more detailed analysis of tanks will be conducted in subsection 3.1.

3 Reverse engineering of propulsion system

As described in subsection 2.3, the propulsion system counts four tanks for storing hydrazine, two tanks for storing NTO and two tanks for storing helium. To better understand the reasoning behind this choice, a reverse sizing for both the propellants and the pressurizer has been conducted given the data on the engines, the ΔV highlighted in Table 2 and the total dry mass M_{dry}[16] of the spacecraft. The whole process has taken into account the standardized margins from ESA.[17] Since the actual mission has greatly deviated from its initial design, a second propellant sizing was also performed on the real manoeuvres up to 7$^{\text{th}}$ June 2021[5][6][18] plus the required de-orbit to check the compliance with the design masses.

3.1 Fuel and oxidizer tanks sizing

1. To estimate the masses of the propellants, Tsiolkovsky rocket equation has been applied iteratively on the ΔV of the first column of Table 2. This process needs the dry mass $M_{dry} = M^{(0)}$ of the spacecraft as first input and starts from the last ΔV (the de-orbit burn) incrementing the computed total mass $M^{(i)}$ and the propellant mass $M^{(i)}_{p,me}$ or $M^{(i)}_{p,rcs}$ after each iteration.

$$M^{(i+1)}_{p,me} = M^{(i)} \cdot \left[\exp\left(\frac{1.05 \cdot \Delta V^{(i)}}{I_{s,me} \cdot g_0} \right) - 1 \right] + M^{(i)}_{p,me} \tag{2}$$

$$M^{(i+1)}_{p,rcs} = M^{(i)} \cdot \left[\exp\left(\frac{2 \cdot \Delta V^{(i)}}{I_{s,rcs} \cdot g_0} \right) - 1 \right] + M^{(i)}_{p,rcs} \tag{3}$$

$$M^{(i+1)} = M^{(i)} + M^{(i)}_{p,me} \qquad \text{or} \qquad M^{(i+1)} = M^{(i)} + M^{(i)}_{p,rcs} \tag{4}$$

where the respective formula is applied based on which engine type performs the i-th manoeuvre.

2. From the final $M_{p,me}$ and $M_{p,rcs}$, the masses of fuel and oxidizer are then computed. This is done by knowing the nominal O/F ratio (0.85) of the ME[9] and that the RCS only uses hydrazine as propellant. Exploiting the density of the propellants, the total volumes for fuel and oxidizer are retrieved.

$$M_f = \frac{1}{O/F + 1} \cdot M_{p,me} + M_{p,rcs} \tag{5}$$

$$M_{ox} = \frac{O/F}{O/F + 1} \cdot M_{p,me} \tag{6}$$

The estimated masses are rather similar to the real ones, as it can be seen in Table 3.

	Estimated masses [kg]	**Real masses [kg][16]**	**Relative error [%]**
M_f	1309.5	1280	2.304
M_{ox}	751.9	752	0.013

Table 3: Comparison between estimated and real masses

3. Having the total volumes of propellants, they have been split among the number of spherical tanks. Since the radius r_{tank} obtained for the two types of tanks are very similar and having two different tanks is inconvenient, the larger one was selected.

Fuel tank radius [cm]	**Oxidizer tank radius [cm]**
43.99	40.91

Table 4: Comparison between obtained radii

4. The pressure of the tanks p_{tank} is kept constant (as described in subsection 2.3). From the pressure and the volume of one tank, the required thickness t_{tank} can be computed by choosing the material, characterized by its density ρ and its tensile yield strength σ.

$$t_{tank} = \frac{r_{tank} p_{tank}}{2\sigma} \tag{7}$$

5. The dry mass of one tank is then computed to select the material:

$$M_{tank} = \frac{4}{3}\pi\rho\left[(r_{tank} + t_{tank})^3 - r_{tank}^3\right] \tag{8}$$

Three different materials have been taken into consideration, and the lighter configuration has been selected.

	Ti6Al4V	**Al7075**	**Stainless steel**
σ **[MPa]**	950	510	1400
ρ **[kg/m^3]**	4500	2810	8100
t_{tank} **[mm]**	0.50	0.93	0.34
M_{tank} **[kg]**	5.45	6.35	6.66

Table 5: Properties of the materials tested for the sizing of the tanks

3.2 Pressurizer tanks sizing

1. As a first approximation, the pressure for the helium tanks is supposed to be ten times the pressure for the propellant tanks p_{tank}, and helium is considered to be a perfect gas (actually it is in a supercritical state). The temperature T_{tank} for the tanks is assumed to be 20 °C. Starting from these assumptions, the mass and the volume

of the total required helium are computed as follows:

$$M_{He} = 1.2 \cdot \frac{p_{tank} \cdot 6V_{tank} \cdot \gamma_{He}}{(1 - 1/10) R_{He} T_{tank}} \tag{9}$$

$$V_{He} = \frac{M_{He} R_{He} T_{tank}}{10 p_{tank}} \tag{10}$$

2. Since the two tanks are cylindrical, the geometry is undefined given only the volume of one tank. To add the missing constraint, a minimization of the total surface is assumed, which can minimize the internal stress due to pressure and the heat transfer through the walls (subsection 2.3).

$$r_{tank,He} = \left(\frac{1/2 V_{He}}{2\pi} \right)^{1/3} \tag{11}$$

$$h_{tank,He} = \frac{1/2 V_{He}}{r_{tank,He}^2 \pi} \tag{12}$$

3. As already done in subsection 3.1, the thickness $t_{tank,He}$ is computed for the materials in Table 5 as:

$$t_{tank,He} = \frac{r_{tank,He} \cdot 10 p_{tank}}{2\sigma} \tag{13}$$

4. The dry mass of one tank is then computed to select the material:

$$M_{tank,He} = \rho \, h_{tank,He} \, \pi \left[(r_{tank,He} + t_{tank,He})^2 - r_{tank,He}^2 \right] + 2 \rho \, t_{tank,He} \, r_{tank,He}^2 \, \pi \tag{14}$$

As for the propellants tanks, titanium alloy appears to be the lightest solution (Table 6). This is the material most likely used for the tanks on the real satellite, and it is the most widely used in space due to its high strength to mass ratio and corrosion resistance.

	Ti6Al4V	**Al7075**	**Stainless steel**
$t_{tank,He}$ **[mm]**	3.58	6.68	2.43
$M_{tank,He}$ **[kg]**	30.62	35.73	37.51

Table 6: Thickness and mass of helium tanks for different materials

3.3 Computation of actual propellants usage

The second sizing relies on the same procedure highlighted in subsection 3.1 with the difference that it starts from the launch mass $M_{launch} = M^{(0)}$[16] and considers the ΔV from the second column of Table 2 in chronological order. Equation 2 and Equation 3 are thus modified as follows:

$$M_{p,me}^{(i+1)} = M^{(i)} \cdot \left[1 - \exp\left(\frac{-\Delta V^{(i)}}{I_{s,me} \cdot g_0} \right) \right] + M_{p,me}^{(i)} \tag{15}$$

$$M_{p,rcs}^{(i+1)} = M^{(i)} \cdot \left[1 - \exp\left(\frac{-\Delta V^{(i)}}{I_{s,rcs} \cdot g_0} \right) \right] + M_{p,rcs}^{(i)} \tag{16}$$

where the ESA margins[17] were not applied since the actually performed manoeuvre values were utilized. The real and consumed masses are reported in Table 7.

	Real masses [kg]	**Consumed masses [kg]**	**Remaining masses [kg]**
M_f	1280	986	294
M_{ox}	752	560	192

Table 7: Real and consumed propellants masses

The *remaining masses* column denotes the propellants masses still present in the spacecraft as of 7th June 2021, which are obtained by subtracting the calculated masses from the real ones. Since the de-orbit is mandatory its ΔV has been considered as a final real manoeuvre even though it hasn't happened yet.

Bibliography

[1] Try Lam Theres D. Kowalkowski. "Launch Period Development for the Juno Mission to Jupiter". In: (2008).

[2] United Launch Alliance. *Atlas V Juno*. Site: https://www.ulalaunch.com/docs/default-source/rockets/atlasvusersguide2010a.pdf?sfvrsn=f84bb59e_2. 2011.

[3] Rick Nybakken. "The Juno Mission to Jupiter: A pre-launch update". In: (2011).

[4] Paul F. Thompson et al. "Juno navigation for Jupiter orbit insertion". In: (2017).

[5] Thomas A. Pavlak et al. *Maneuver Design for the Juno Mission: Inner Cruise*. AIAA space forum. Site: https://arc.aiaa.org/. 2018.

[6] Paul W. Stumpf et al. *Maneuver Operations During Juno's Approach, ORBIT INSERTION, AND EARLY ORBIT PHASE*. JPL open repository. Site: https://dataverse.jpl.nasa.gov/file.xhtml?fileId=58768&version=1.1&toolType=PREVIEW. 2017.

[7] S. Stephens. *Juno Mission Plan Document*. Planetary Data System. Site: https://pds.nasa.gov/ds-view/pds/viewMissionProfile.jsp?MISSION_NAME=JUNO. 2011.

[8] Various. *Juno Mission and Trajectory Design*. Website. Site: https://spaceflight101.com/juno/juno-mission-trajectory-design/. 2024.

[9] Nammo. *Leros 1b engine*. Journal of Geophysical Research: Planet. Site: https://www.nammo.com/wp-content/uploads/2021/03/2021-Nammo-Westcott-Liquid-Engine-LEROS1B.pdf.

[10] Dr. Edward. J. Wucherer al. *Improving and Testing S-405 Catalyst*. AIAA space forum. Site: https://arc.aiaa.org/doi/epdf/10.2514/6.2013-4053. 2013.

[11] *Aerojet Rocketdyne Propulsion plays role in Juno mission*. Online Communication. Site: https://www.proquest.com. 2016.

[12] *MR-111C datasheet*. Site: http://www.astronautix.com/m/mr-111.html.

[13] *Launch*. Site: https://www.missionjuno.swri.edu/launch.

[14] Dr. Mary M. Mellott et al. *NSSDCA/COSPAR ID: 2011-040A*. Nasa SSDCA. Site: https://nssdc.gsfc.nasa.gov/nmc/spacecraft/display.action?id=2011-040A. 2022.

[15] Sathya Gangadharan et al. *Modeling of Fuel Slosh in a Spin Stabilized Spacecraft with On-Axis Propellant Tanks Implemented with Diaphragms*. AIAA Modeling and Simulation Technologies Conference 10 - 13 August 2009, Chicago, Illinois. Site: https://arc.aiaa.org/. 2009.

[16] NASA JPL. *Juno Quick Facts*. Site: https://www.jpl.nasa.gov/news/press_kits/juno/facts/. 2011.

[17] European Space Agency. "Margin philosophy for science assessment studies". In: (2012).

[18] Thomas A. Pavlak et al. "Juno trajectory redesign following PRM cancellation". In: (2017).